Contract No:

This document was prepared in conjunction with work accomplished under Contract No. DE-AC09-08SR22470 with the U.S. Department of Energy (DOE) Office of Environmental Management (EM).

Disclaimer:

SRNL-L4400-2018-00017
Revision 0

July 30, 2018

To: B. L. García-Díaz

From: M. J. Martínez-Rodríguez

Management Approval: M. M. Reigel, Materials Science & Technology Date

Status of the Full Circumference Examination of the Inner Container Closure Weld Region for Selected 3013 DE Containers

Summary

One of the main focus areas of the 3013 Surveillance Program is a thorough evaluation of the inner container closure weld region (ICCWR) opened for destructive examination (DE). As part of the protocol to investigate the corrosion in the ICCWR a laser confocal microscope (LCM) is used to perform close visual examination of the surface and measurements of corrosion features on the surface. In FY17, DE containers from FY13 through FY16 were evaluated to select candidates for a full circumference analysis of the ICCWR. In FY18, the selected DE containers for full circumference evaluation (FCE) were processed according to the ICCWR protocol. However, due to the time intensive task for collecting high magnification images for a full circumference, only FY15 DE07 was selected for completion of LCM data collection in FY18 with the remaining DE containers scheduled to be completed in FY19.

The ICCWR protocol was completed as follows: (1) the FCE containers were sectioned into quarters and the weld removed to access the ICCWR; (2) a series of images of the ICCWR full circumference were taken using a stereo microscope and assembled into panoramic views; (3) SEM/EDS analysis performed on selected sections showed what is most likely corrosion products on the surface and chlorides randomly dispersed; (4) the presence of chlorides was also confirmed with ion chromatography of citric acid washes, in which FY15 DE07 and FY16 DE05 showed a significant amount of chlorides with FY15 DE08 showing the less amount of chlorides; (5) dye penetrant examination was performed on the interior and exterior surfaces of all the sidewall sections but reveled no relevant indication of surface-breaking defects, (6) finally, as described above, only FY15 DE07 was selected for completion of the full circumference examination of the ICCWR by LCM.

The data collected for FY15 DE07 showed general and localized corrosion on the surface. This includes noticeable surface loss from areas were the tint of the heat affected zone disappeared, rougher surface compared to the baseline container, as well as pits scattered throughout the surface or clustered in small regions. Also, two major suspect corrosion events were observed. This corresponds to one crack found in Section C1 and another found in Section C2. Both cracks were found at the boundary of Zone 2 and Zone 3 extending upward and downward from a large and deep pit. The vertical length of the cracks in Sections C1 and C2 was measured as 640 μm and 1080 μm, respectively. The maximum pit depth associated with each crack and that can be measured with the LCM is 66 μm and 68 μm, respectively. These cracks are

close to the region of maximum residual stresses and are very similar to those produced during the boiling $MgCl_2$ tests conducted at SRNL. High humidity and chloride content were present in this DE container which are ideal conditions for crack development. However, gas analysis and statistical evaluation of the gas compositions and pressures via GEST analyses suggest that leakage between the outer/inner (OI) and inner container (IC) volumes was unlikely. Additional characterization and analysis will be performed on the locations where the cracks were found.

Introduction

The 2014 test plan for assessing the potential of stress corrosion cracking (SCC) of the 3013 inner container was issued by the Materials Identification and Surveillance (MIS) Corrosion Working Group to determine if SCC is plausible within the 50-year design life of a 3013 storage container [1]. One of the main focus areas is a thorough evaluation of the inner container closure weld region (ICCWR) opened for destructive examination (DE), which is part of the 3013 Surveillance Program. A protocol to investigate the corrosion in the ICCWR was developed to characterize the type of corrosion (i.e., mechanisms), the extent of corrosion (percentage of area and depth of attack) and the variables impacting this corrosion (chloride concentration and metallurgical condition) [2, 3]. Figure 1 shows an overview of the protocol for the examination of the ICCWR, which includes some updated steps from the original version [4]. The steps include (1) the sectioning of the inner container lid into easily handled pieces and weld removal, (2) low-magnification imaging of the entire circumference of the ICCWR, (3) surface analysis of selected pieces using Scanning Electron Microscope (SEM) and Energy Dispersive Spectroscopy (EDS), (4) chemical analysis of selected pieces using wet chemistry techniques, (5) dye penetrant examination of exterior surfaces, (6) further sectioning of selected pieces into 1/8 can sections in preparation for LCM analysis, (7) cleaning selected pieces for removing corrosion products using nitric acid, (8) surface depth profiling and high-magnification imaging of the cleaned pieces with identified corroded areas within the ICCWR using LCM, and (9) serial metallography of pieces as necessary. Results from this characterization are used to assign a corrosion categorization to the respective ICCWR.

As part of the ICCWR examination protocol, a Keyence 3D laser confocal microscope (LCM) model VK-X110 is used to perform close visual examination of the surface at the ICCWR and surface profile measurements for pit depths or other corrosion features on the surface. Initial analysis of selected DE containers using the LCM revealed several challenges for acquiring, processing and interpreting the data [4, 5]. These challenges include topography of the ICCWR sample, surface features, and the amount of surface area for collecting data at high magnification conditions. Consequently, the LCM parameters were investigated by imaging several samples with known cracks of different sizes to identify the appropriate parameter values for data acquisition and identification of regions of interest. Using these parameter values, selected DE containers were analyzed to determine the extent of the ICCWR to be examined. These parameters and conditions have been defined and reported in FY17 [6].

DE containers from FY13 through FY16 were evaluated to select candidates for a full circumference analysis of the ICCWR. This information will be used to perform a statistical analysis with Los Alamos National Laboratory (LANL) that will help support a determination of how much of an ICCWR needs to be examined in order to make the assertion of whether or not cracking has occurred and develop an ICCWR sampling plan for analysis of subsequent containers. In FY17, the following DE containers were selected for full circumference analysis of the ICCWR with the following prioritization order: FY15 DE07, FY16 DE05, and FY15 DE08 [6].

In FY18 the selected DE containers for full circumference analysis were processed according to the ICCWR protocol described above. However, due to the time intensive task for collecting high magnification images for a full circumference, only FY15 DE07 was selected for completion of LCM data collection in FY18 with the remaining DE containers scheduled to be completed in FY19. This report describes the results obtained from the ICCWR protocol for the selected DE containers and the LCM images for the full circumference of FY15 DE07.

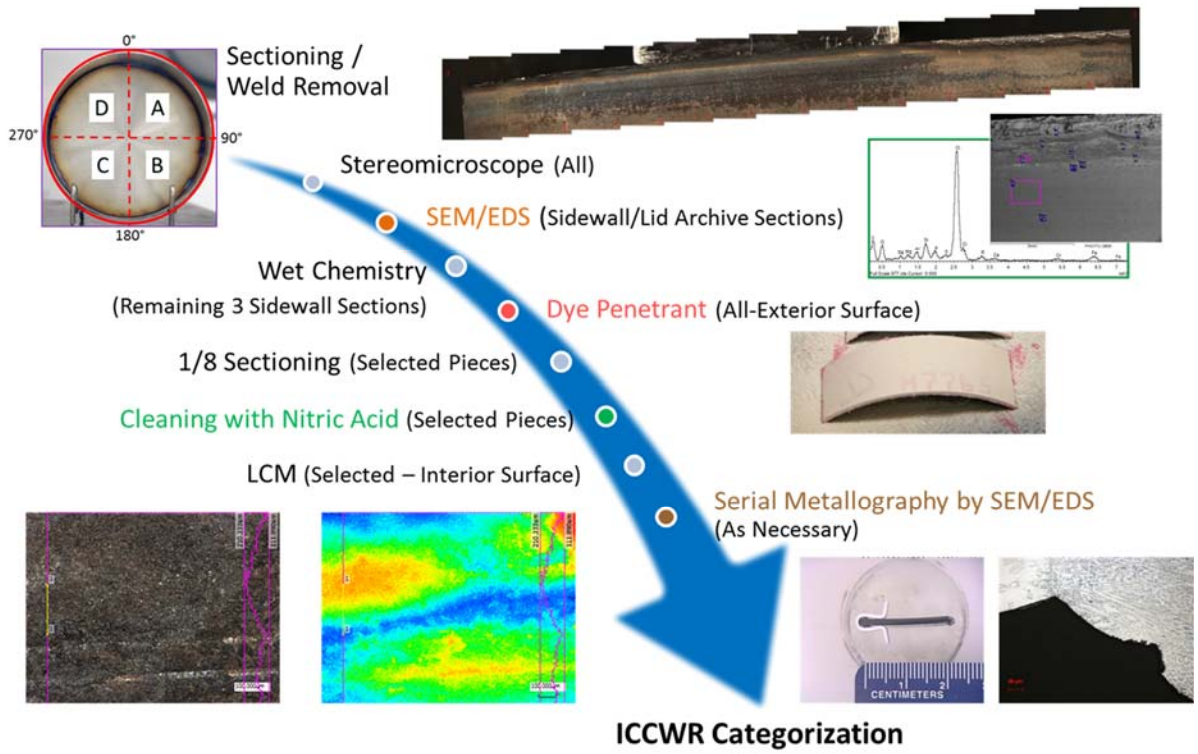

Figure 1. Protocol overview for the examination of the ICCWR.

ICCWR Examination for Selected DE Containers

The protocol as described above was completed for FY15 DE07, FY16 DE05, and FY15 DE08. For simplicity, this set of DE containers are referred as the full circumference evaluation (FCE) containers. From these FCE containers, high magnification images for a full circumference were obtained only for FY15 DE07. Also, under normal circumstances, an archive piece is selected for determining surface chloride distribution within the ICCWR using SEM/EDS while the remaining quarter pieces are used to quantify the chloride concentration using wet chemistry techniques. In this case, all pieces, including the one selected as archive, are needed to make the ICCWR full circumference. Consequently, all the quarter pieces were used for chloride quantification. FY15 DE07 was examined by LCM in FY18 while the remaining DE containers will be examined in FY19. Analysis by serial metallography is determined on as needed basis.

Panoramic Images of the ICCWR by Stereomicroscope

The FCE containers were sectioned into quarters and the weld removed from each section as described in previous reports [4-6]. However, the current nomenclature for the quarter sections follows a clockwise direction starting from the weld overlap (defined as 0°) when facing the interior of the inner container lid as shown in Figure 1. The reason for this direction is because it follows the direction in which the weld was made. Note that past DE containers that were opened followed the nomenclature base on the exterior of the inner container [5].

Once the weld was removed and the lid and sidewall separated, a series of images of the now accessible ICCWR were taken using the stereo microscope. These images were assembled into a panoramic view for each section lid and sidewall. These panoramic views of the ICCWR are shown in Figure A.1 through Figure A.6 for the FCE containers. Technical issues during the weld removal of FY16 DE05 Section D caused the loss of part of the ICCWR as shown in Figure A.4. It was estimated that about 6% of the ICCWR area was lost based on the 6 mm analysis in Zone 3 [6]. It was determined by the MIS Working Group that this container will still be analyzed as scheduled. All the sections show corrosion in the ICCWR.

SEM and EDS Analysis

From the sidewall quarter sections of the FCE containers, one quarter section of each container was selected for analysis by SEM/EDS. These sections were selected as the ones showing more corrosion based on the 35 mm pictures of the inner containers lids [6] and the stereo microscope images shown in Appendix A. These sections correspond to FY15 DE07 Section C, FY16 DE05 Section C and FY15 DE08 Section A and are denoted “archive” sections. SEM images, EDS point scans and EDS map of the chloride on the surface are shown for each selected section in Figure 2 through Figure 7.

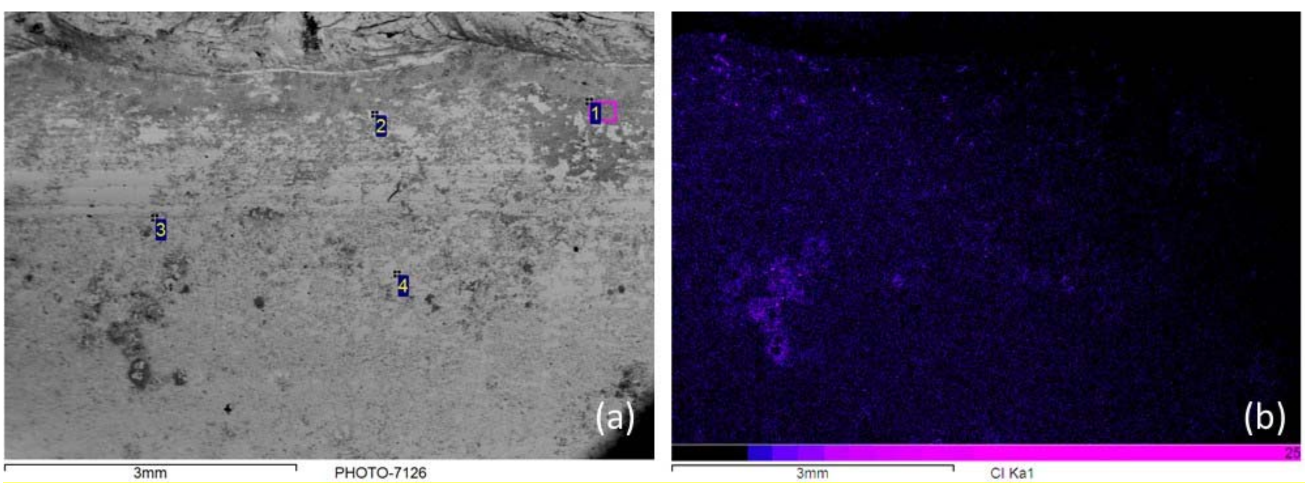

Figure 2. Surface image of Zones 1, 2 and 3 within Section C for FY15 DE07 by (a) SEM and (b) EDS map of Cl.

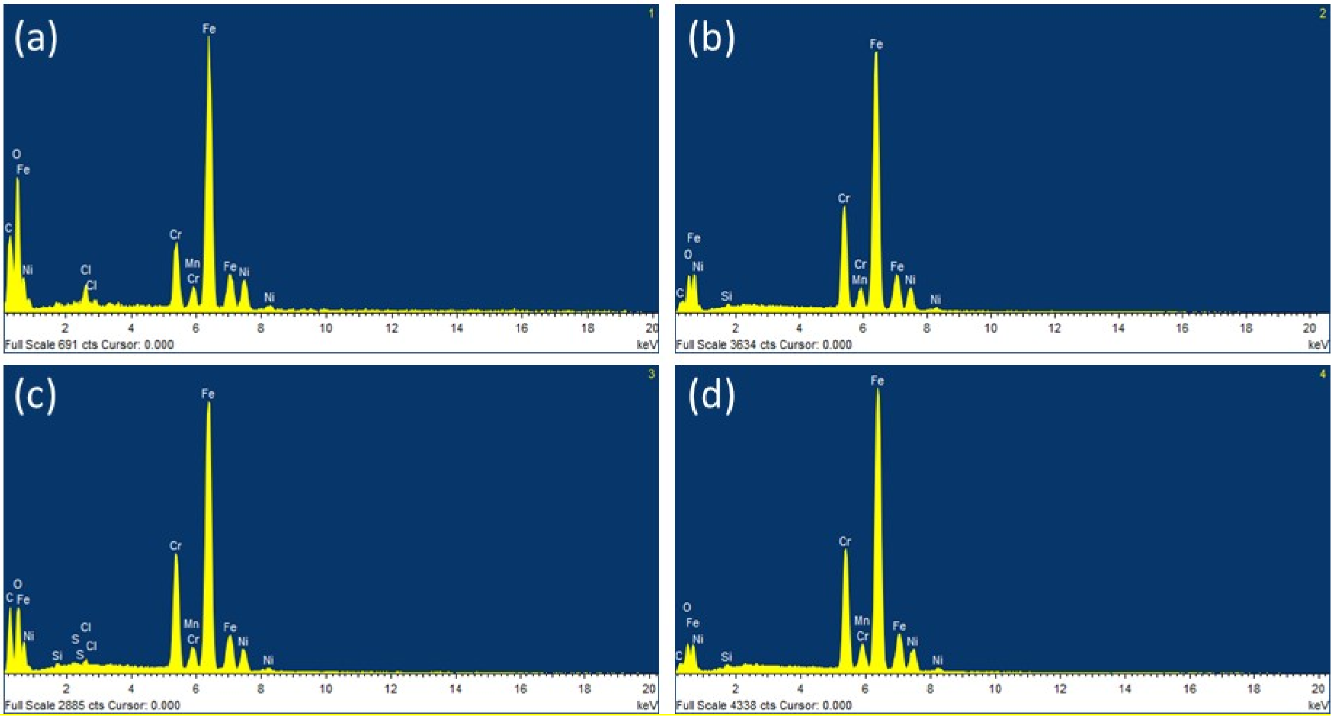

Figure 3. EDS point scans for FY15 DE07 for the image shown in Figure 2(a). Points 1, 2, 3 and 4 correspond to (a), (b), (c) and (d) respectively.

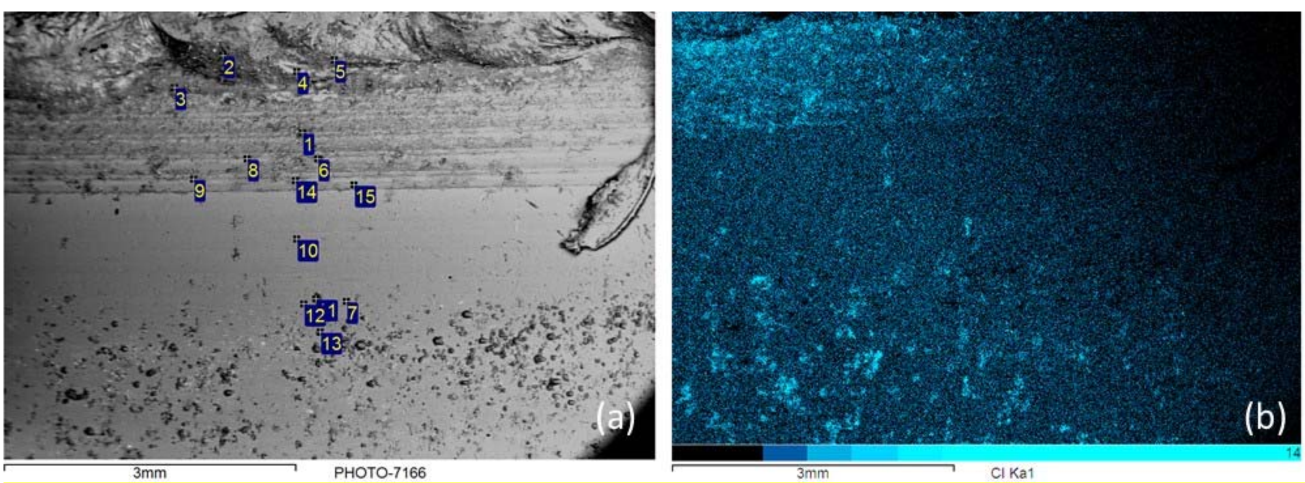

Figure 4. Surface image of Zones 1, 2 and 3 within Section C for FY16 DE05 by (a) SEM and (b) EDS map of Cl.

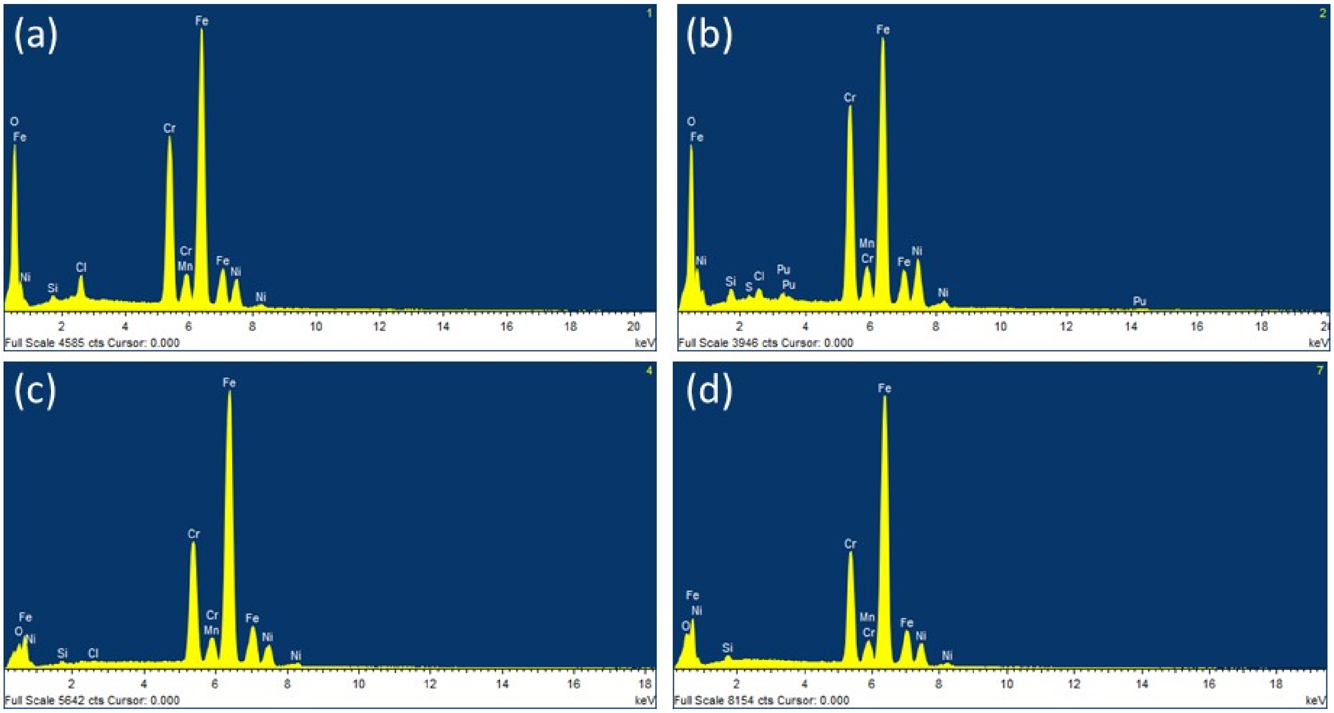

Figure 5. Selected EDS point scans for FY16 DE05 for the image shown in Figure 4(a). Points 1, 2, 4 and 7 correspond to (a), (b), (c) and (d) respectively.

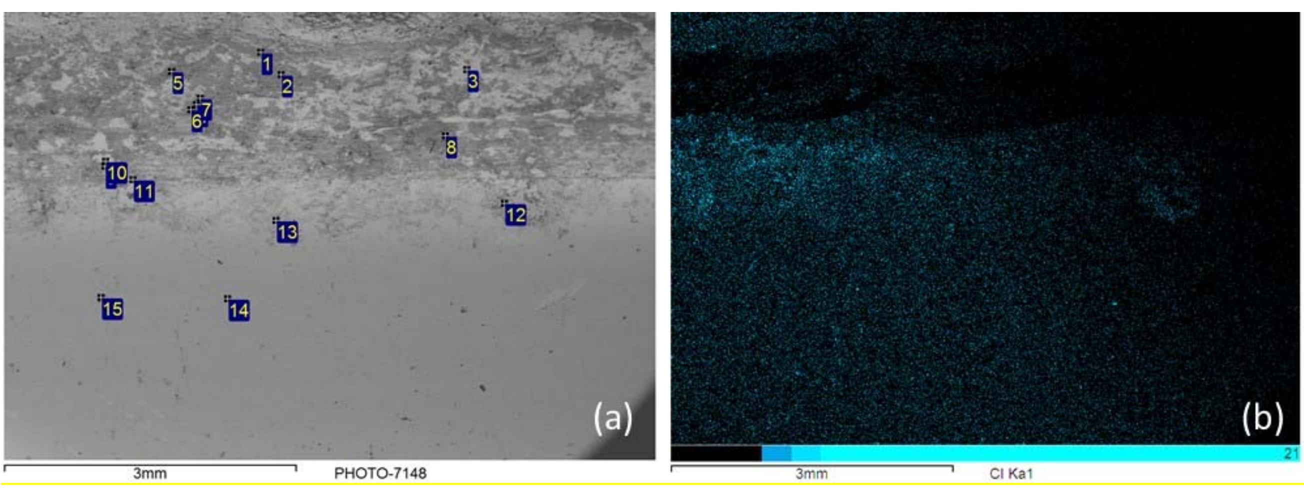

Figure 6. Surface image of Zones 1, 2 and 3 within Section A for FY15 DE08 by (a) SEM and (b) EDS map of Cl.

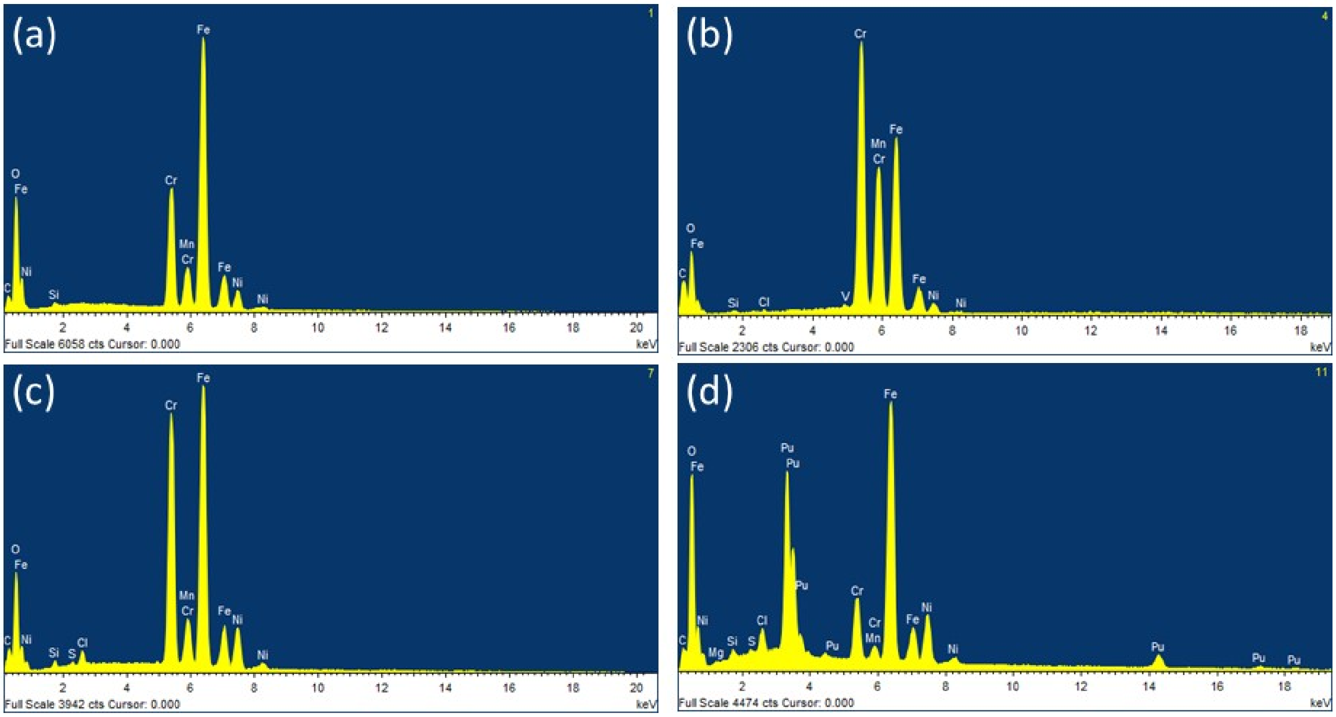

Figure 7. Selected EDS point scans for FY15 DE08 for the image shown in Figure 6(a). Points 1, 4, 7 and 11 correspond to (a), (b), (c) and (d) respectively.

SEM images of a portion of the sidewall sections of these FCE container show what is most likely corrosion products on the surface. An EDS map of the chloride on the surface for each FCE container show that the amount of chlorides varies with location and that the chlorides are randomly dispersed over the surface. This is reflected on the EDS point scans at several locations which show different intensities for the chloride peak.

Chloride Quantification

Chloride removal from the ICCWR was performed by washing the surface of each sidewall quarter section with 10 wt% citric acid at 60°C for 60 min using sonication. The first wash was performed by covering Zones 1 and 2 as shown in Figure 8 followed by a second wash in Zones 1 – 3. For the "archive" sections three washes were performed in Zones 1 – 3 in order to determine how many washes are required to remove the chlorides. The results for the chloride concentration on each section are shown in Table 1. Table 2 shows the results after normalizing for the approximate surface area of the washed zones.

FY15 DE07 and FY16 DE05 show a significant amount of chlorides with FY15 DE08 showing the less amount of chlorides. Also, the three washes in Zones 1 – 3 show a decrease in the amount of chlorides with each wash, suggesting that additional washes may be necessary to remove all the chlorides.

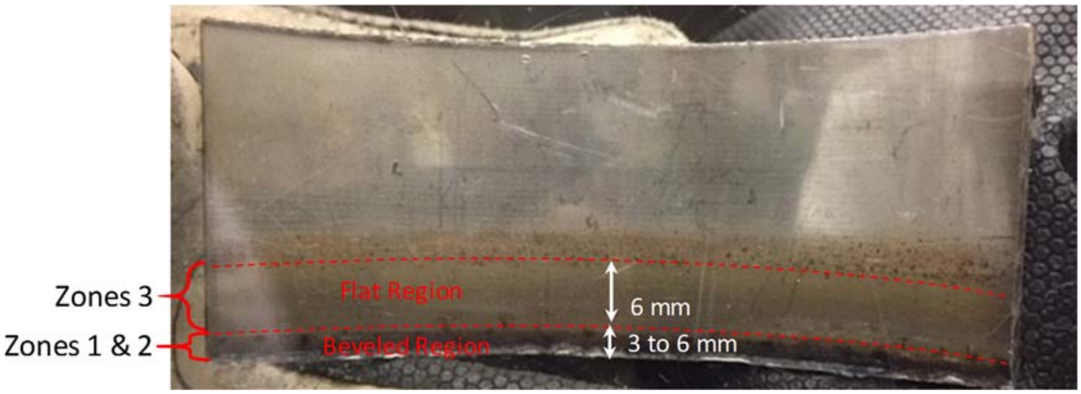

Figure 8. Typical sidewall quarter section showing Zones 1 and 2 (beveled region) and Zone 3 (flat region). of the ICCWR.

Table 1. Chloride concentration in μg/mL from washes performed on the sidewall sections of the FCE containers.

Inner Container Sample ID	Chloride concentration (μg/mL)			
	1st Wash		2nd Wash	3rd Wash
	(Zones 1-2)	(Zones 1-3)	(Zones 1-3)	(Zones 1-3)
FY15 DE07				
Section A	15.50		3.78	
Section B	13.30		3.83	
Section C		12.50	4.56	2.94
Section D	11.40		3.90	
FY16 DE05				
Section A	10.60		< 1.50	
Section B	17.20		3.57	
Section C		43.9*	13.40	4.45
Section D	6.66		< 1.50	
FY15 DE08				
Section A		3.63	1.36	< 1.00
Section B	2.79		< 1.50	
Section C	3.42		1.06	
Section D	4.14		< 1.50	

* Analysis error may have occurred. Reported for completeness.

Table 2. Chloride concentration in μg/mm^2 from washes performed on the sidewall sections of the FCE containers.

Inner Container Sample ID	Chloride concentration (μg/mm^2)			
	1st Wash		2nd Wash	3rd Wash
	(Zones 1-2)	(Zones 1-3)	(Zones 1-3)	(Zones 1-3)
FY15 DE07				
Section A	0.174		0.021	
Section B	0.149		0.022	
Section C		0.070	0.026	0.017
Section D	0.128		0.022	
FY16 DE05				
Section A	0.119		< 0.008	
Section B	0.193		0.020	
Section C		0.247*	0.075	0.025
Section D	0.075		< 0.008	
FY15 DE08				
Section A		0.020	0.008	< 0.006
Section B	0.031		< 0.008	
Section C	0.038		0.006	
Section D	0.047		< 0.008	

* Analysis error may have occurred. Reported for completeness.

Dye Penetrant Examination

Dye penetrant examination was performed on the interior and exterior surfaces of the sidewall sections of the FCE containers. The method utilized for the dye penetrant test is described in details in reference [4]. The test was performed by a Penetrant Inspector – Level III. Figure 9 through Figure 11 show the dye penetrant test results. These examinations revealed no relevant indication of surface-breaking defects. The stain in the developer, as shown in Figure 11 for FY15 DE08 Section A, that seems to match on the interior and exterior surface, was determined to be a mark on both sides due to handling during sectioning of the inner container lid.

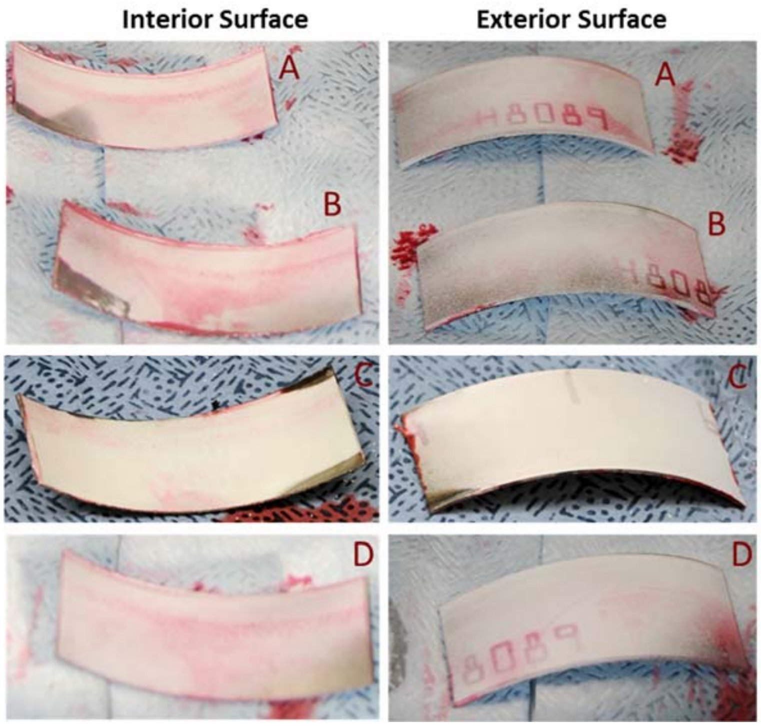

Figure 9. Dye penetrant test for the inside and outside surfaces of the sidewall sections of FY15 DE07.

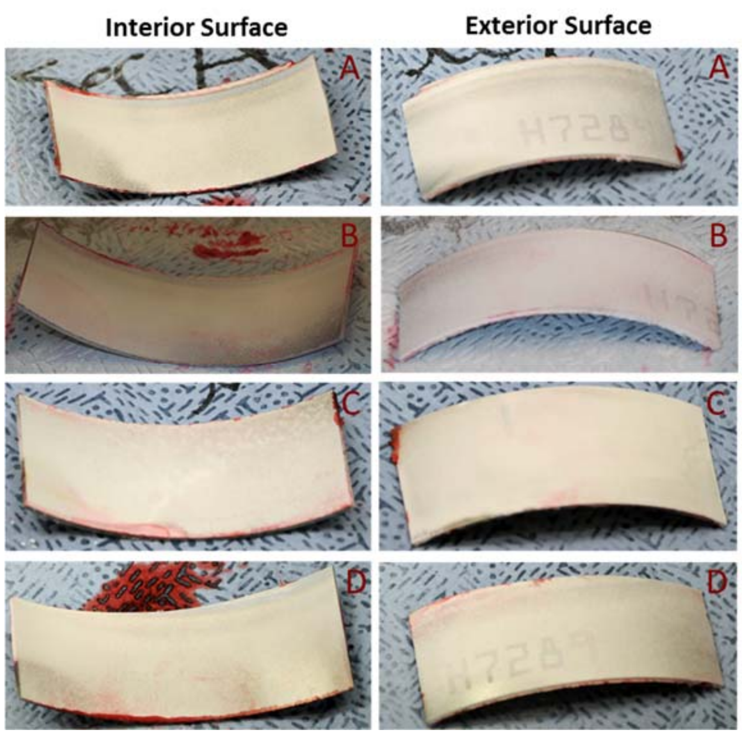

Figure 10. Dye penetrant test for the inside and outside surfaces of the sidewall sections of FY16 DE05.

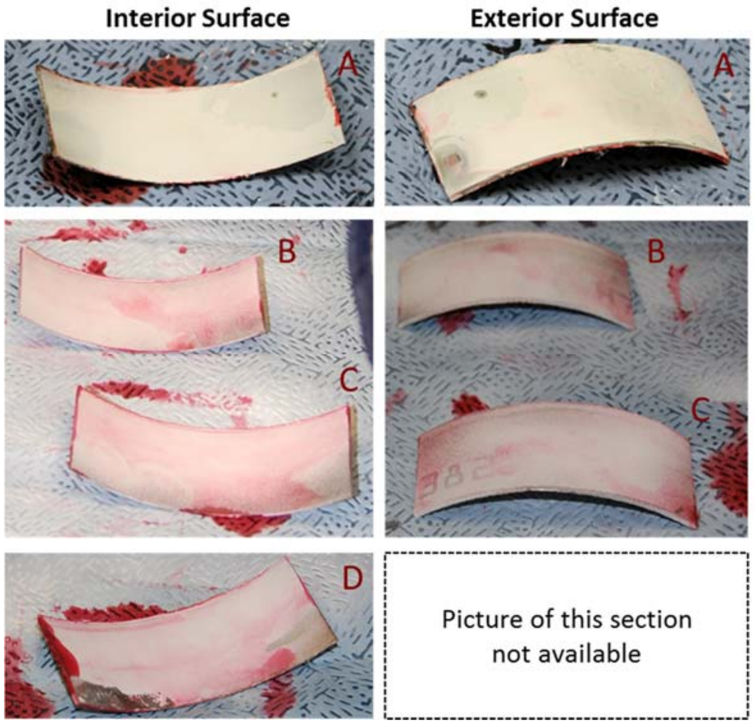

Figure 11. Dye penetrant test for the inside and outside surfaces of the sidewall sections of FY15 DE08.

ICCWR Full Circumference Examination by LCM of FY15 DE07

As described above, only FY15 DE07 was selected for completion of the full circumference examination of the ICCWR by LCM in FY18 with the remaining DE containers scheduled to be completed in FY19. Sample preparation for LCM included (1) cutting 1/4 sections (A, B, C and D) into 1/8 sections of the container lid to reduce the curvature of each sidewall piece to be scanned and to fit the sample in the sample holder box (LCM box); (2) cleaning the samples from corrosion products using 2.0 M nitric acid solution and sonication for 60 min at 60°C; (3) mounting each 1/8 section into the LCM box minimizing tilt as much as possible. Detailed sample preparation is described in previous report [4].

The LCM parameters used to collect data for the full circumference were determined in FY17 and are discussed in details in reference [6]. The parameters set during the data collection were the image magnification, measurement area (refers to x-y directions in pixels), quality (related to the laser speed), and pitch (refers to the spacing resolution in the z-direction). These parameters were selected for the examination of the ICCWR with detection of cracks of, at least, 1 µm. Image and height data were collected on Zone 3 of the ICCWR using 20X magnification, with the double scan function disabled, measurement area set to standard, quality set to high accuracy, and a pitch value of 0.5 µm. The vertical extent of the data collection in Zone 3 was 6 mm (see Figure 8). Zones 1 and 2 were examined but images or height data were not collected unless areas of interest were found. These areas of interest correspond to sections where suspect cracks, significant number of pits or other corrosion features are located. However, due to the difficulty for observing a curved surface in real time because most of the surface is out-of-focus while a portion is in-focus, many of the sections have data collected in the full circumference of Zones 1 and 2. Data collection for Zones 1 and 2 used the same parameters as Zone 3, except the double scan function was enabled.

These optical data for the ICCWR full circumference of FY15 DE07 is shown in Figure B.1 through Figure B.8 in Appendix B. Each figure shows the set of assemblies that comprise the total for 1/8 section of the container. Each 1/8 container section was generally divided into 14 sub-sections for data collection because of the curvature nature of the sample in the x-direction. Figure 12 shows the sample orientation in the LCM box and axis directions with representative curvatures and slopes for Zone 3 and steeper slopes in Zones 1 and 2. The exceptions to the division into 14 sub-sections were Section A1, which was used initially to test and define the length of each sub-section, and Section B1 which was longer than the instrument stage x-range and needed an extra sub-section. As shown in Figure 13, the steeper the subsection (towards the outside edges) the longer it takes to collect data and, consequently, the smaller the sub-section was defined to expedite the data collection. Conversely, the flatter the subsection (towards the center) the shorter it takes to collect data and the larger the sub-section was able to be defined. The length of the sub-sections was established such that the total vertical distance (Δz) was maintained approximately 1,600 μm microns or less as shown in Figure 14.

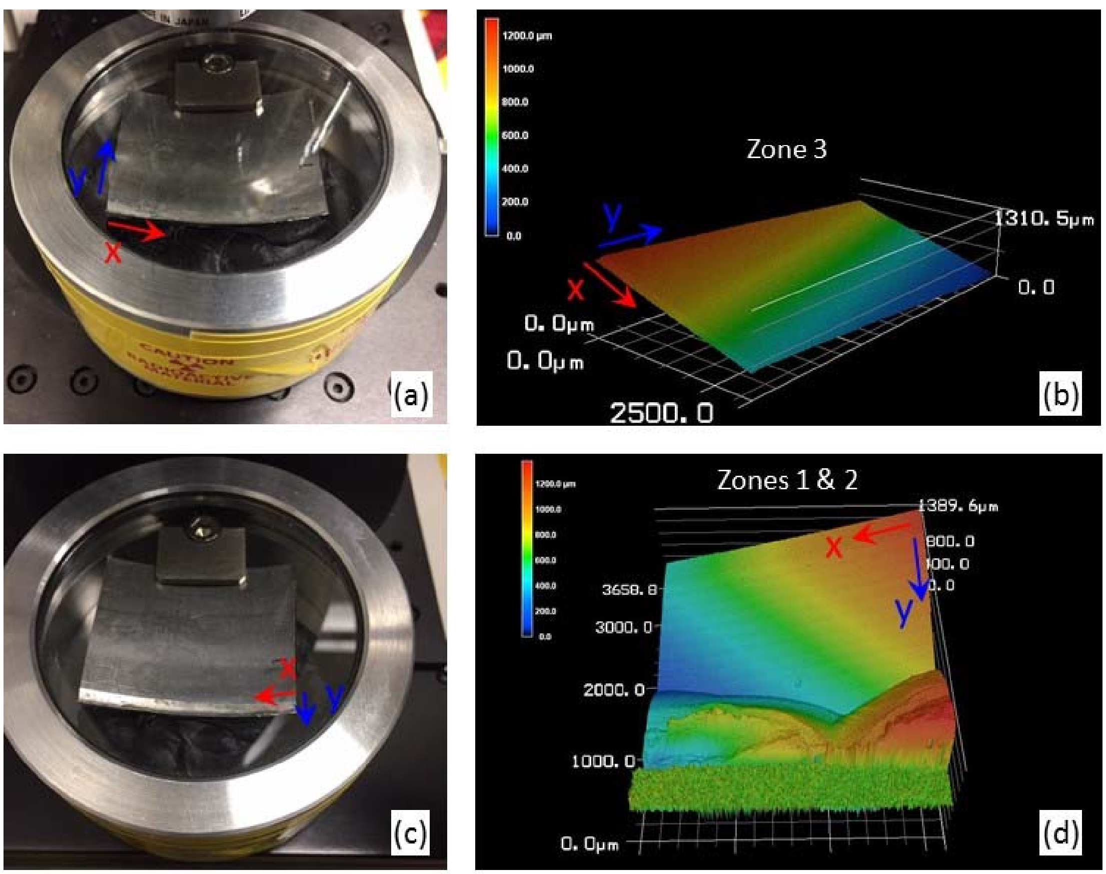

Figure 12. Sample orientation showing the x and y-directions for FY15 DE07 Section A2 mounted in (a) LCM box and (b) 3D representation of the surface of Zone 3 (Sub-section 4); and for FY15 DE07 Section A1 mounted in (c) LCM box and (d) 3D representation of the surface of Zones 1 and 2 (near Sub-section 7).

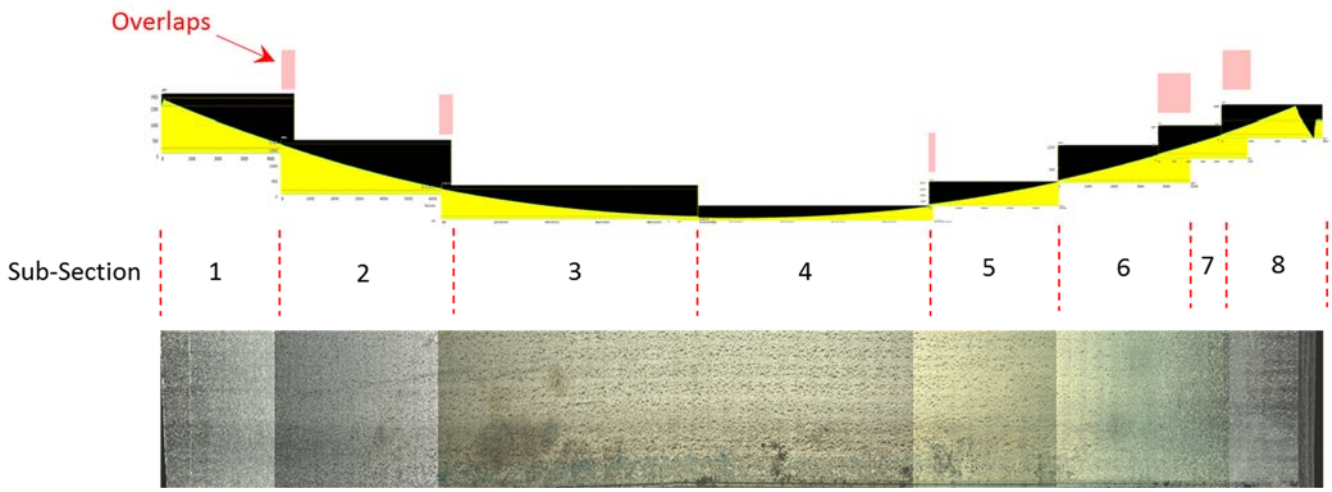

Figure 13. Cross-section profile of the sidewall of FY15 DE07 Section A1 (top) showing curvature of the sample and Zone 3 panoramic assembly (bottom) of sub-sections.

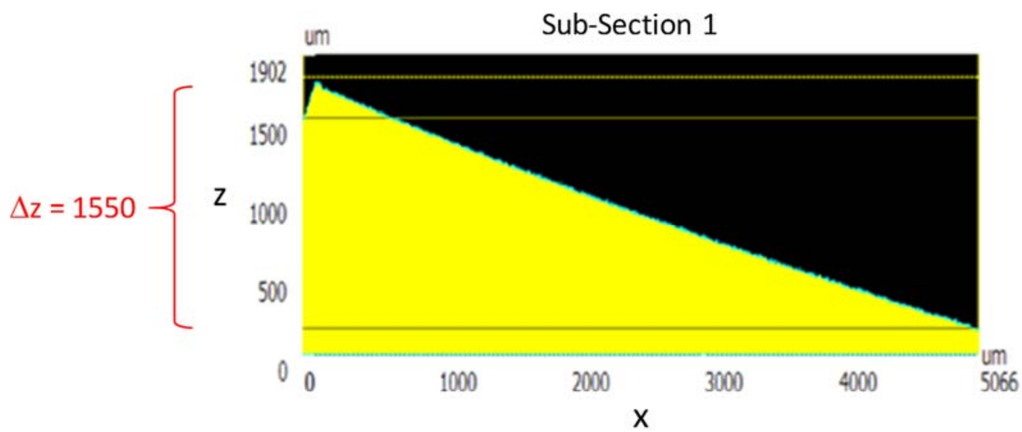

Figure 14. Cross-section profile of Sub-Section 1of the sidewall of FY15 DE07 Section A1.

LCM data collection of high magnification images, height and laser intensity data for the full circumference of the ICCWR is a time intensive task with large number of images and amount of data. Also, as discussed above, the curvature of the sample (in the x-direction) and the tilt (in the x and y-direction) increases the data collection time because it increases the range in the z-direction that the instrument needs to scan and focus the image. For Zone 3, center and larger sub-sections took about 3 – 4 hrs to complete while outer and smaller sub-sections took 10-14 hrs. For Zones 1 and 2 the double scan feature had to be utilized due to the steeper slope nature in these zones. Consequently, the time to complete the selected sections in these zones was between 5 hrs for very small sections up to 48 hr for larger sections. It required approximately 4 months to complete the full circumference, including overnight time. Table 3 shows a summary of the total images collected for each sub-section of FY15 DE07. An average of 1,166 images were collected per sub-section for a total of 9,330 images in Zone 3. An additional 2,233 images were collected in Zones 1 and 2.

Table 3. Number of LCM images collected for the sub-sections of FY15 DE07.

DE Sub-Section	Number of Images	
	Zones 1 & 2	Zone 3
A1	104	1,125
A2	202	1,215
B1	232	1,380
B2	185	960
C1	616	1,230
C2	340	1,185
D1	318	1,050
D2	236	1,185
Total	**2,233**	**9,330**

As the LCM data was collected, the images assemblies were visually inspected for signs of corrosion and cracks. This allowed obvious corrosion features to be found on the surface, but it does not provided a through and detailed analysis of the individual images. Analysis of the individual images is cumbersome, and it requires more sophisticated computer analysis, such as the Machine Learning approach. This type of approach is in process of development and will be utilized in the future to perform a detailed analysis of the data collected.

The data collected for FY15 DE07 shows general and localized corrosion on the surface. This includes noticeable surface loss from areas were the tint of the heat affected zone disappeared, rougher surface compared to the baseline container, as well as pits scattered throughout the surface or clustered in small regions. Also, two major suspect corrosion events were observed. This corresponds to one crack found in Section C1 and another found in Section C2. The crack found in Section C1 is shown in Figure 15. This crack was found at the boundary of Zone 2 and Zone 3 extending upward and downward from a large and deep pit. The vertical length of the crack that can be observed from the optical image is approximately 640 μm with its widest opening of about 25 μm. Height scan data shown in Figure 16 indicates that the area around the crack contains pits scattered throughout the surface. Also, the horizontal linear profile (A-B) in Figure 16(b) shows that the maximum depth of the pit that can be measured with the LCM is 66 μm. A vertical linear profile (C-D) along the crack is shown in Figure 16(c). Various depths were measured between 20 μm and 42 μm. Additional LCM data will be collected at higher magnifications on the location of the crack and at the outer surface of the sample and opposite side of the crack. However, in order to determine a more accurate depth for the crack and extent of it, serial metallography and SEM/EDS analysis of sample cross-sections around the crack will be performed.

The second crack found was observed on Section C2. This crack was also found at the boundary of Zone2 and Zone 3 extending upward and downward from a large and deep pit as shown in Figure 17. The vertical length of the crack that can be observed from the optical image is approximately 1080 μm. In addition, this crack shows indication of crack branching as pointed by the white arrows in Figure 17(c). Height scan data and linear profiles are shown in Figure 18. The horizontal linear profile (A-B) in Figure 18(b) shows that the maximum depth of the pit that can be measured with the LCM is 68 μm. A vertical linear profile (C-D) along the crack show various depths between 18 μm and 29 μm as shown in Figure 18(c). Additional characterization will be performed for this crack as well.

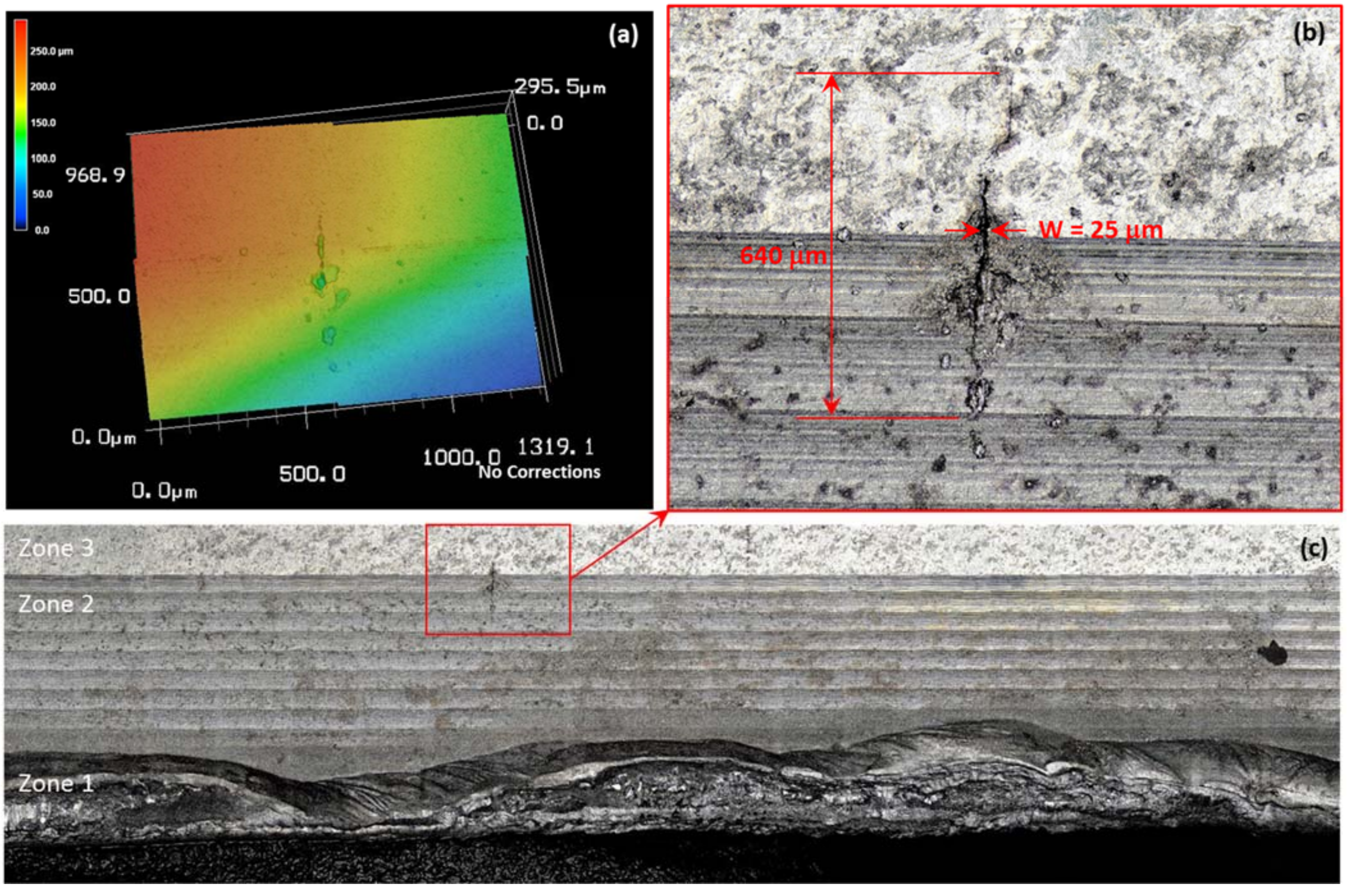

Figure 15. LCM analysis for the area of the sidewall of FY15 DE07 Section C1 where a crack was found showing (a) the top view of the 3D representation of the surface, (b) the optical image zoom of the crack shown in (c) the optical image of Zones 1 – 3.

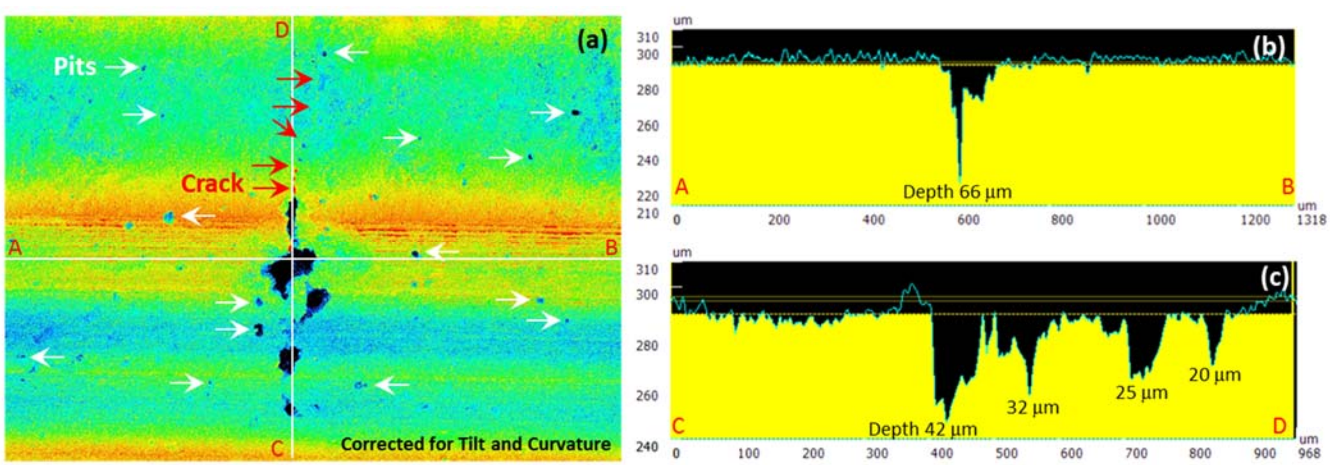

Figure 16. LCM analysis for the area of the sidewall of FY15 DE07 Section C1 where a crack was found showing (a) the height scan for the image in Figure 15(b). Increasing height is represented by transition in color from blue (lowest) to red (highest). White arrows in height scan correspond to pit locations. White lines (A-B and C-D) in height scan show positions of (b) horizontal line profile and (c) vertical line profile.

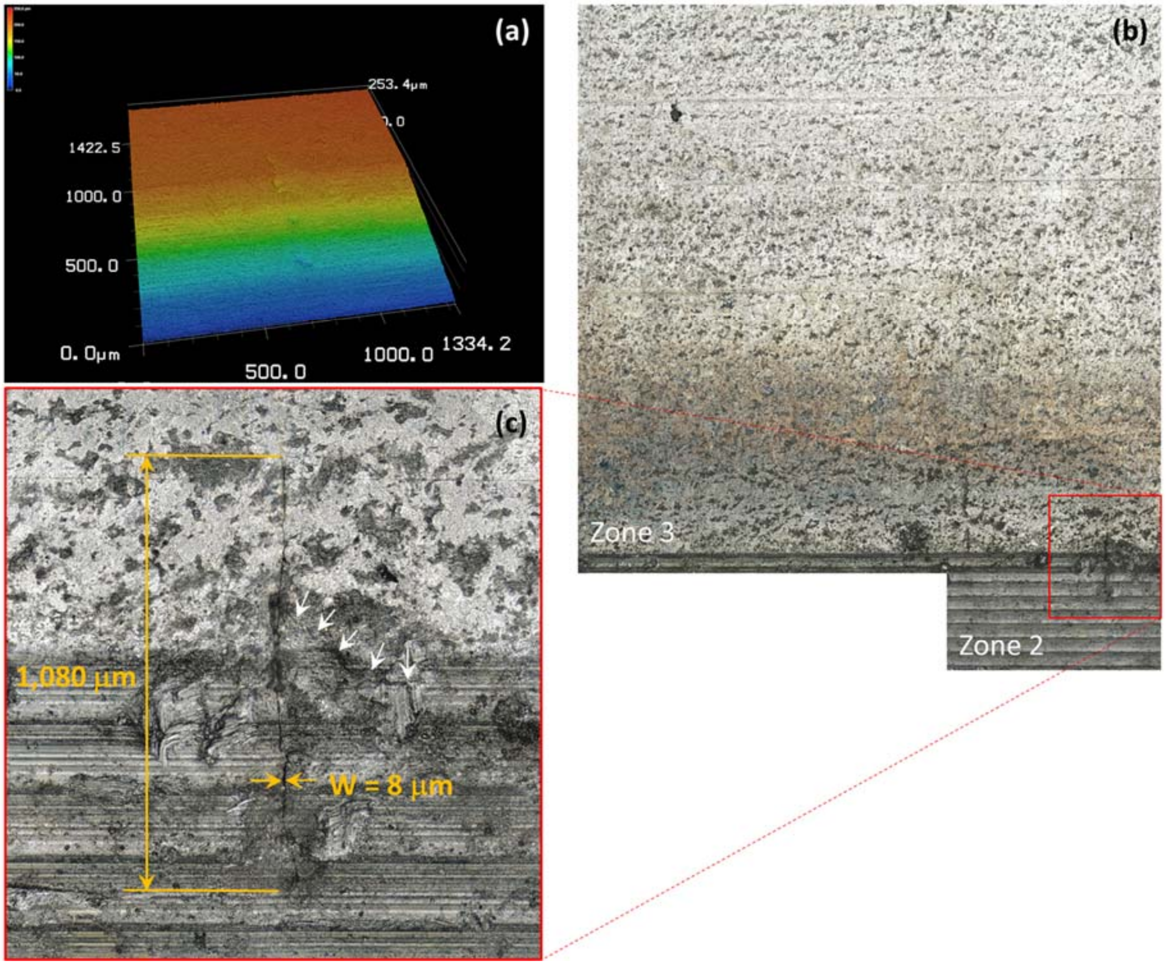

Figure 17. LCM analysis for the area of the sidewall of FY15 DE07 Section C2 where a crack was found showing (a) the top view of the 3D representation of the surface, (b) the optical image of Zones 2 – 3 where the crack was found and (c) the optical image zoom of the crack.

The FY15 DE07 container was selected for surveillance by engineering judgment due to the high moisture value (0.24%). In addition, analysis of the Pu oxide by ionic chromatography reveled a high content of chlorides (80,231 μg/g). The presence of chlorides in the ICCWR is clearly shown in the EDS results discussed in this report and confirmed by ion chromatography of the critic acid washes of the quarter sections. Hence, the conditions for crack development were present. Furthermore, the cracks described above were found at the boundary of Zone2 and Zone 3, which is close to the region of maximum residual stresses [6, 7]. Note that the images of the cracks are very similar to those produced during the boiling $MgCl_2$ tests conducted at SRNL [8, 9]. Figure 19 shows an optical image with the cracks produced from the boiling $MgCl_2$ test. However, gas analysis and statistical evaluation of the gas compositions and pressures via GEST analyses suggest that leakage between the OI and IC volumes was unlikely [10].

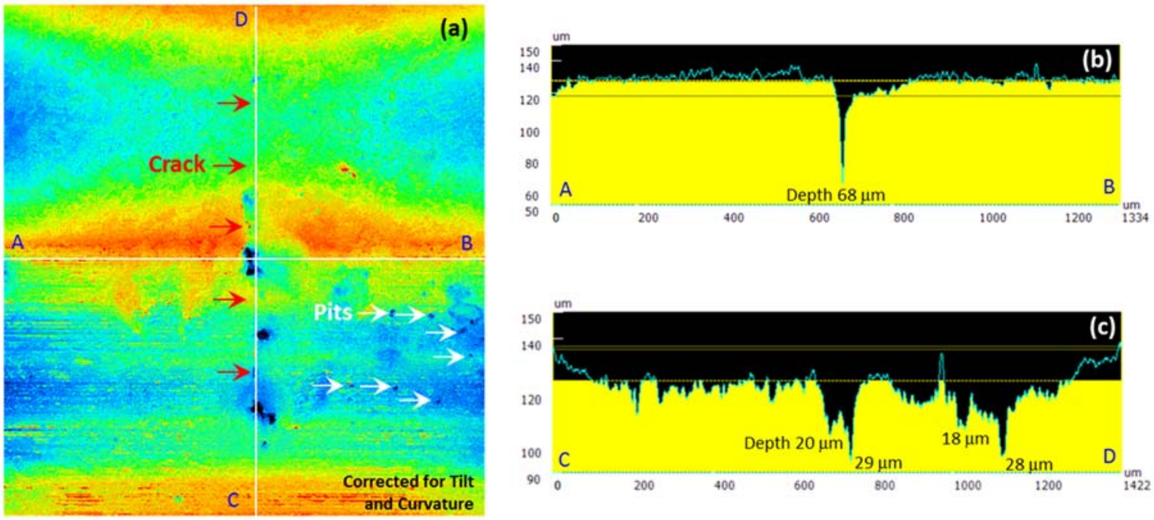

Figure 18. LCM analysis for the area of the sidewall of FY15 DE07 Section C2 where a crack was found showing (a) the height scan for the image in Figure 15(b). Increasing height is represented by transition in color from blue (lowest) to red (highest). White arrows in height scan correspond to pit locations. White lines (A-B and C-D) in height scan show positions of (b) horizontal line profile and (c) vertical line profile.

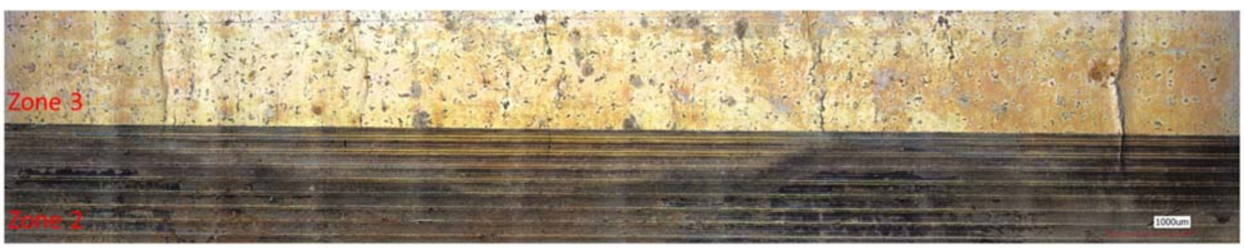

Figure 19. Optical image of ICCWR sidewall Zones 2 and 3 of DE container from boiling $MgCl_2$ test. Note that the picture is oriented such that the weld is below Zone 2 [6].

Conclusions and Future Work

Corrosion evaluation of three prioritized DE containers, selected from candidates between FY13 and FY16, was performed for the ICCWR full circumference. The selected DE containers for full circumference evaluation (FCE) correspond to the following prioritization order: FY15 DE07, FY16 DE05, and FY15 DE08. These DE containers were processed according to the ICCWR protocol. However, due to the time intensive task for collecting high magnification images for a full circumference, LCM data collection was completed only for FY15 DE07 while the remaining DE containers are scheduled to be completed in FY19.

The ICCWR protocol was completed as described in this paragraph. The FCE containers were sectioned into quarters and the weld removed from each section to access the ICCWR. A series of images of the ICCWR full circumference were taken using a stereo microscope and assembled into a panoramic view. From the sidewall quarter sections, one quarter section of each container was selected for analysis by SEM/EDS. SEM images showed what is most likely corrosion products on the surface while an EDS map of the chloride on the surface for each FCE container show that the chlorides are randomly disperse. The presence of chlorides was confirmed with ion chromatography of acid washes, in which FY15 DE07 and FY16 DE05 show a significant amount of chlorides with FY15 DE08 showing the less amount of chlorides. Dye penetrant examination was performed on the interior and exterior surfaces of all the sidewall sections. These examinations reveled no relevant indication of surface-breaking defects. Finally, as described above, only FY15 DE07 was selected for completion of the full circumference examination of the ICCWR by LCM. The FY15 DE07 samples were cut into 1/8 sections of the can lid and cleaned from corrosion products. The LCM parameters were defined in FY17 for the examination of the ICCWR with detection of cracks of, at least, 1 μm. The vertical extent of the data collection in Zone 3 was 6 mm. It required approximately 4 months to complete the full circumference, including overnight time. A total of 9,330 images were collected in Zone 3 with an additional 2,233 images collected in Zones 1 and 2.

The data collected for FY15 DE07 shows general and localized corrosion on the surface. This include loss of surface noticeable from areas were the tint of the heat affected zone has disappeared, rougher surface compared to the baseline container, pits scattered throughout the surface of clustered in small regions. Also, two major suspect corrosion events were observed. This corresponds to one crack found in Section C1 and another found in Section C2. Both cracks were found at the boundary of Zone 2 and Zone 3 extending upward and downward from a large and deep pit. The vertical length of the cracks in Sections C1 and C2 was measured as 640 μm and 1080 μm, respectively. The maximum pit depth associated with each crack and that can be measured with the LCM is 66 μm and 68 μm, respectively. These cracks are close to the region of maximum residual stresses and are very similar to those produced during the boiling $MgCl_2$ tests conducted at SRNL. High humidity and chloride content were present in this DE container which are ideal conditions for crack development. However, gas analysis and statistical evaluation of the gas compositions and pressures via GEST analyses suggest that leakage between the OI and IC volumes was unlikely.

Additional characterization will be performed on the locations where the cracks were found. LCM data will be collected at higher magnifications on the location of the cracks and at the outer surface of the sample and opposite side of the cracks. Also, in order to determine a more accurate depth and extent of the cracks, serial metallography and SEM/EDS analysis of sample cross-sections around the crack will be performed. For the analysis of the individual LCM images, a Machine Learning approach is in development and it will be utilized in the future to perform a detailed analysis of the data collected.

Acknowledgements

The assistance and efforts of Gregg Creech, Vickie Timmerman, Thaddeus Reown, Kellie Hair, Lisa Ward, Roc Seabrook, and Jason Corley are acknowledged in the execution of this protocol.

References

1. Berg, J.M., D.K. Veirs, E.J. Kelly, Juan G. Duque, S.A. Joyce, J.E. Narlesky, J.M. Duffey, J.I. Mickalonis, and K.A. Dunn, *Test Plan for Assessing Potential for Stress Corrosion Cracking in the 3013 Inner Container Closure Weld Region (FY 2014).* 2014, LA-UR-14-20785.
2. Mickalonis, J.I., *3013 DE Inner Container Closure Weld Corrosion Evaluation.* 2013, SRNL-STI-2013-00527.
3. Mickalonis, J.I. and K.A. Dunn, *Protocol for Examination of the Inner Can Closure Weld Region for 3013 DE Containers.* 2014, SRNL-L4400-2014-00020.
4. Martínez-Rodríguez, M.J., *Status of the Examination of the Inner Container Closure Weld Region for Selected 3013 DE Containers.* 2016, SRNL-L4400-2016-00021.

5. Mickalonis, J.I. and G.T. Chandler, *Status of the Examination of the Inner Container Closure Weld Region for FY13 and FY14 3013 DE Containers.* 2015, SRNL-L4400-2015-00020.
6. Martínez-Rodríguez, M.J., *Laser Confocal Microscope for Analysis of 3013 Inner Container Closure Weld Region.* 2017, SRNL-STI-2017-00589.
7. Stroud, M.A., M.B. Prime, D.K. Veirs, J.M. Berg, B. Clausen, L.A. Worl, and A. DeWald, *Assessment of Residual Stresses in 3013 Inner and Outer Containers and Teardrop Samples.* 2015, LA-UR-15-29376.
8. Mickalonis, J.I., *Assessment of Residual Stresses in SRS and Hanford 3013 Inner and Convenience Cans.* 2009, SRNL-STI-2009-00121.
9. Mickalonis, J.I. and K.A. Dunn, *Residual Stresses in 3013 Containers.* Journal of Nuclear Materials Management, 2010, **38**: p. pp 31-38.
10. Hardy, B.J., *Evaluation of 2013-2016 KIS Data for Gas Composition and Pressure in the Inner and Outer 3013 Containers.* 2017, SRNL-STI-2017-00490.

Appendix A

Panoramic Assemblies of Stereomicroscope Images of ICCWR Sections

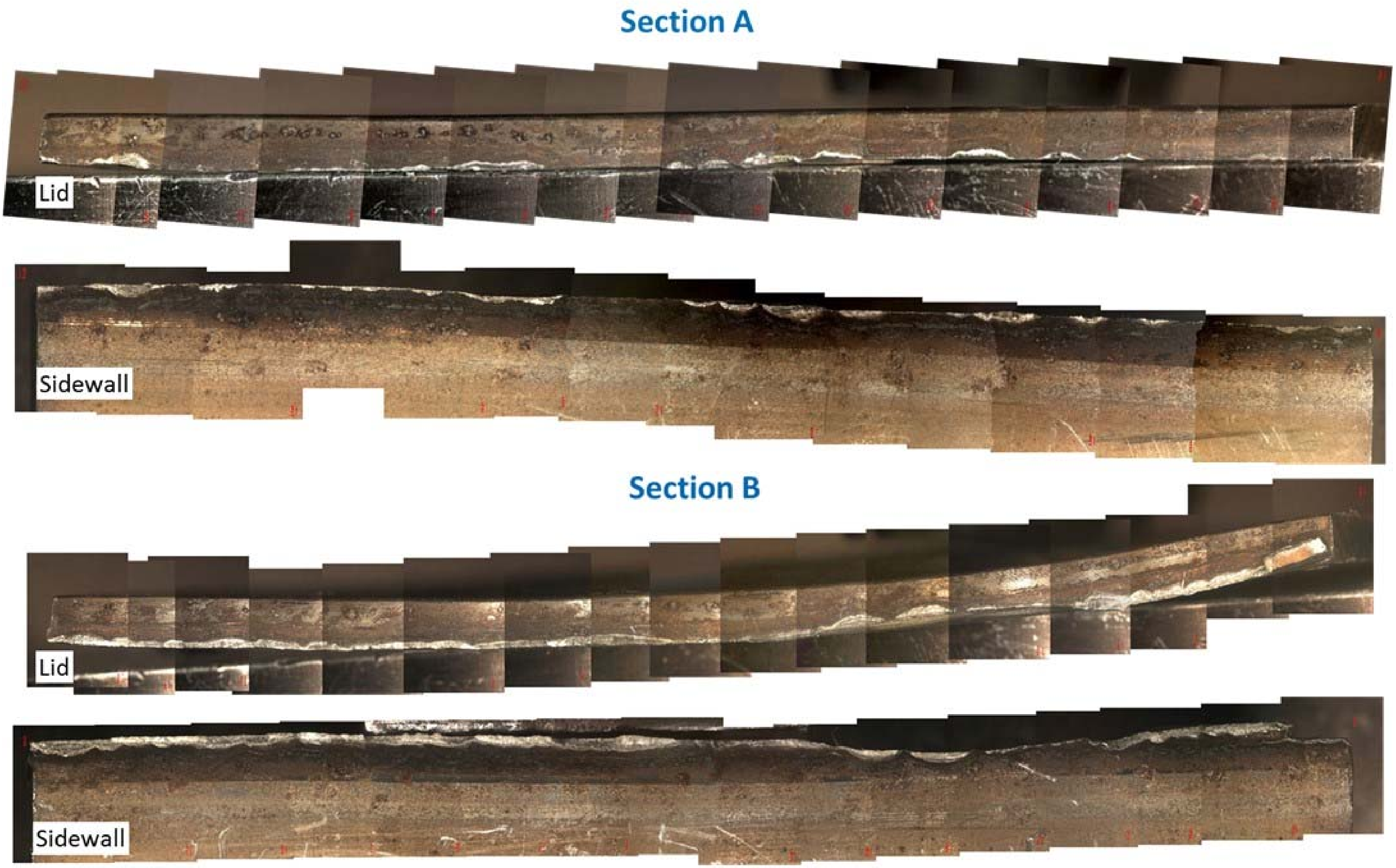

Figure A.1. Panoramic assembly of stereomicroscope images of ICCWR for FY15 DE07 Sections A and B.

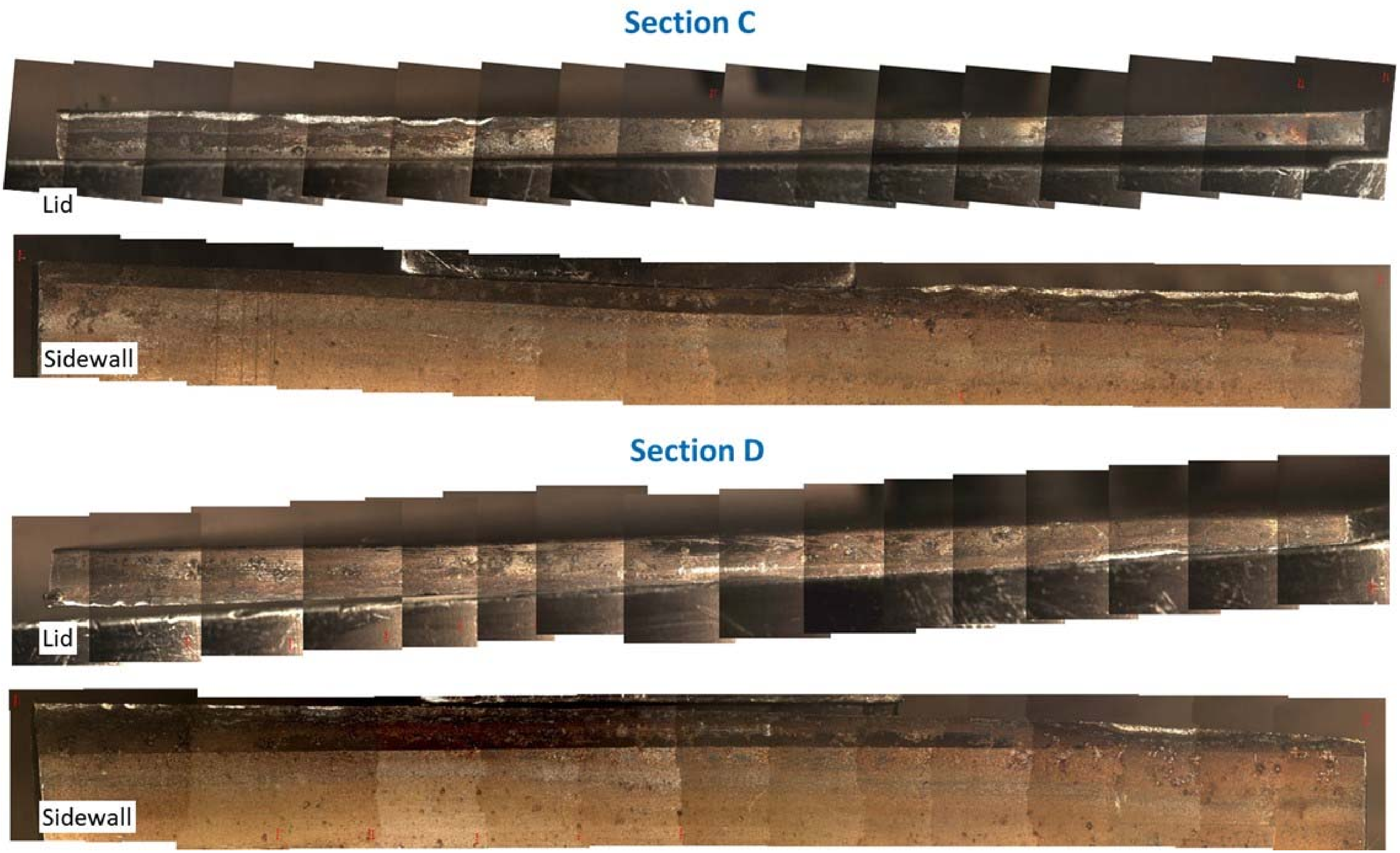

Figure A.2. Panoramic assembly of stereomicroscope images of ICCWR for FY15 DE07 Sections C and D.

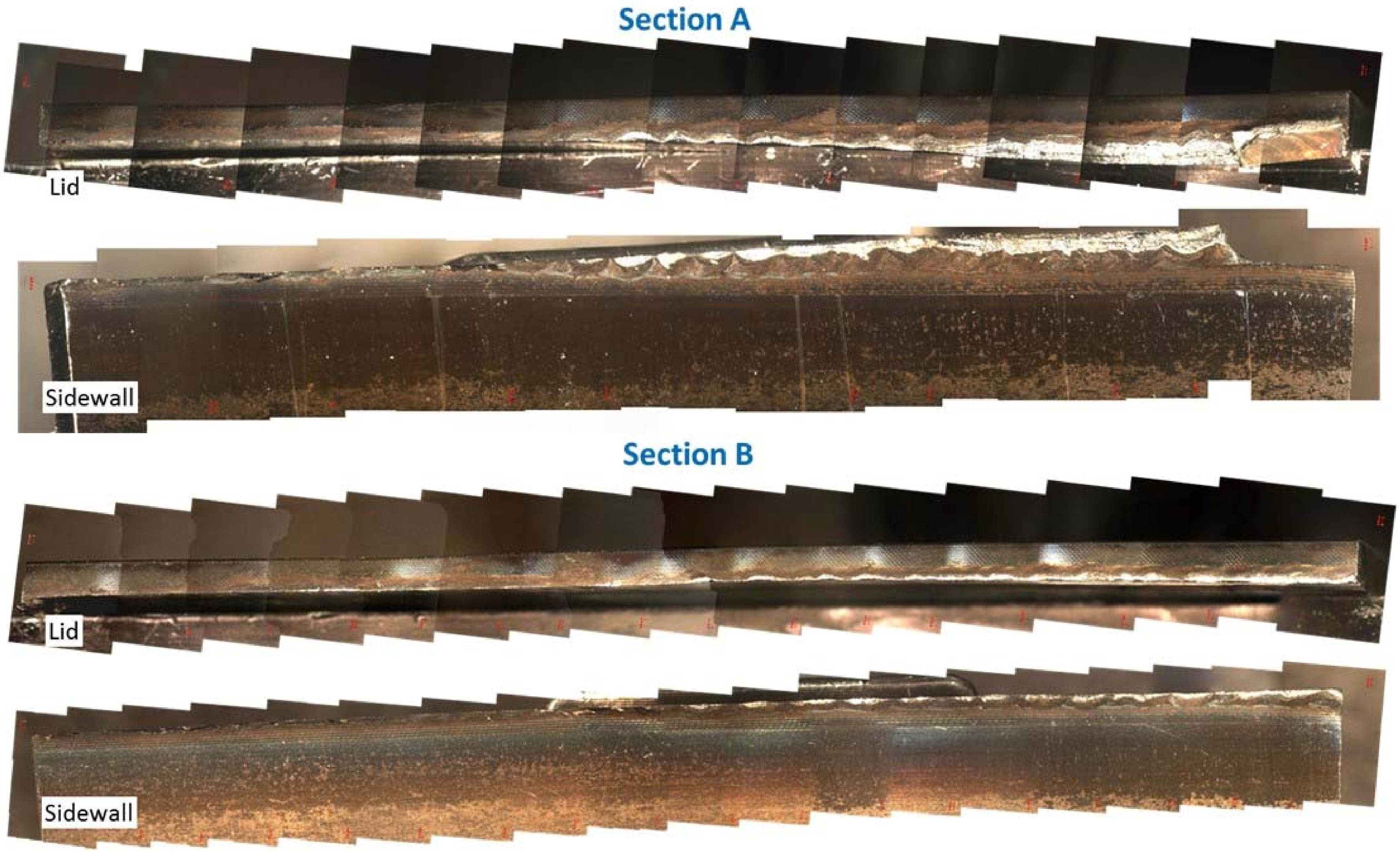

Figure A.3. Panoramic assembly of stereomicroscope images of ICCWR for FY16 DE05 Sections A and B.

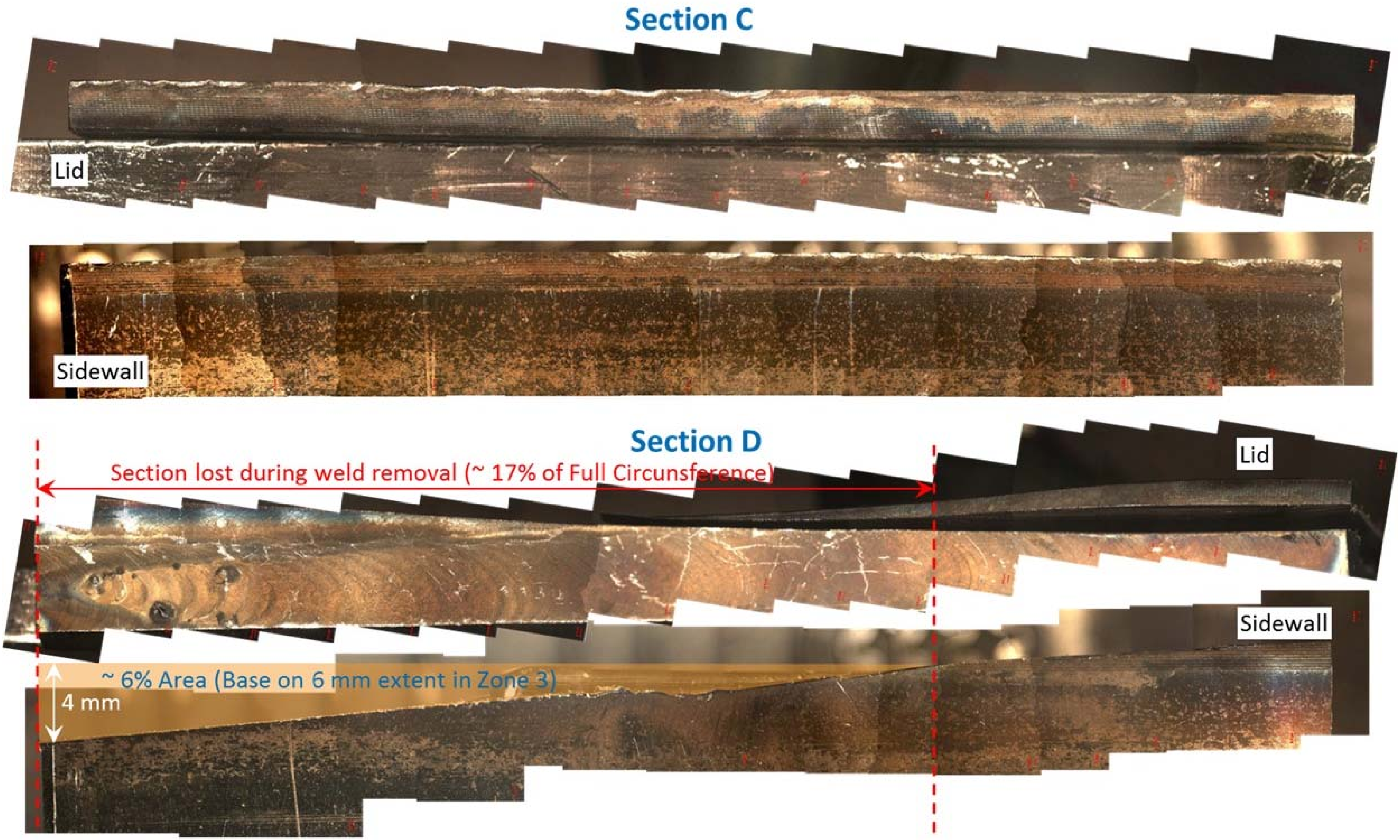

Figure A.4. Panoramic assembly of stereomicroscope images of ICCWR for FY16 DE05 Sections C and D.

Figure A.5. Panoramic assembly of stereomicroscope images of ICCWR for FY15 DE08 Sections A and B.

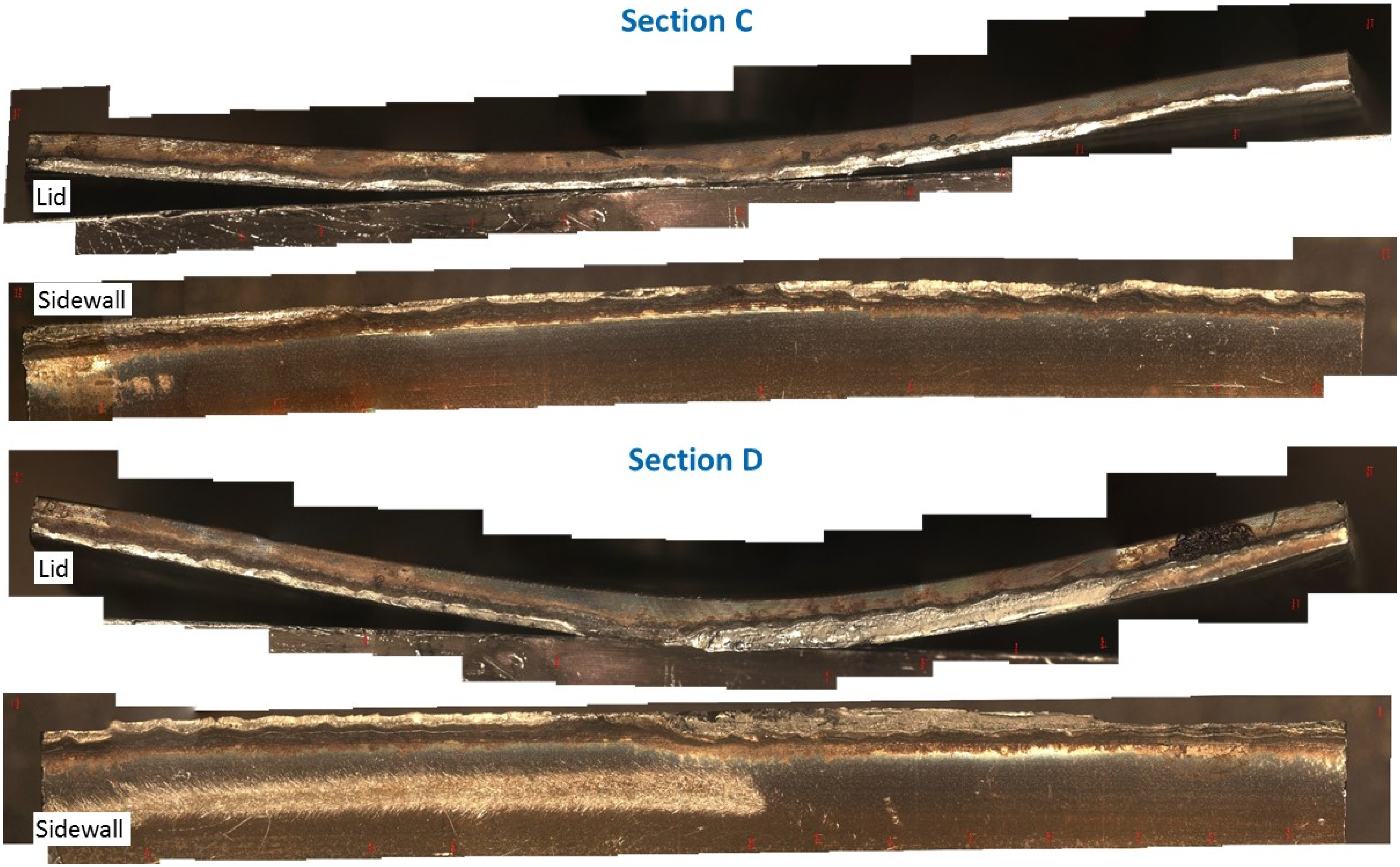

Figure A.6. Panoramic assembly of stereomicroscope images of ICCWR for FY15 DE08 Sections C and D.

Appendix B

Assemblies of Laser Confocal Microscope Images of ICCWR Sidewall Sections of FY17 DE05

Figure B.1 Side by side LCM assemblies of Zone 3 (top) and Zones 1 and 2 (bottom) of ICCWR for FY15 DE07 Section A1. Zone 1 corresponds to the weld beads, Zone 2 corresponds to the machining marks region (above weld beads), and Zone 3 is the region above the machining marks. Each image represents an assembly of 75 to 240 individual images. Some overlap exits between assemblies to ensure data collection of 100% of full circumference.

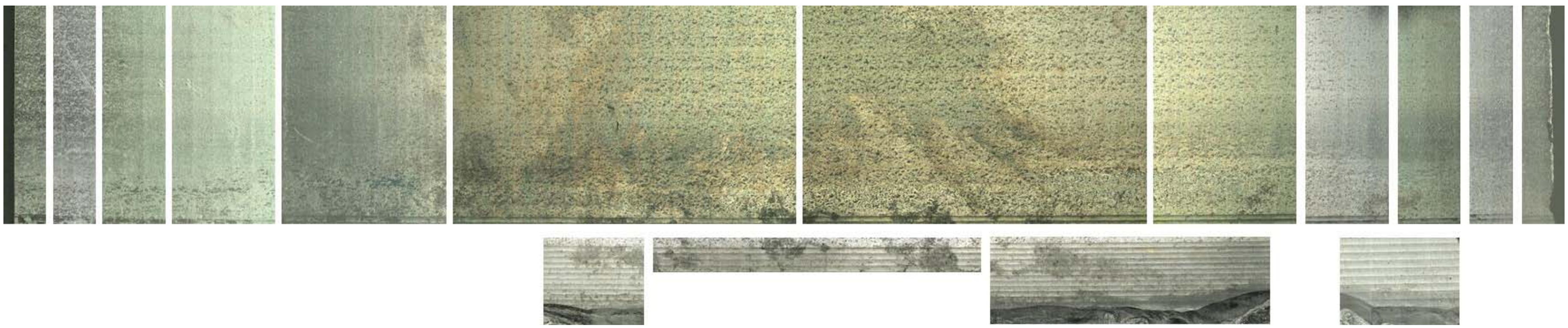

Figure B.2 Side by side LCM assemblies of Zone 3 (top) and Zones 1 and 2 (bottom) of ICCWR for FY15 DE07 Section A2. Zone 1 corresponds to the weld beads, Zone 2 corresponds to the machining marks region (above weld beads), and Zone 3 is the region above the machining marks. Each image represents an assembly of 30 to 255 individual images. Some overlap exits between assemblies to ensure data collection of 100% of full circumference.

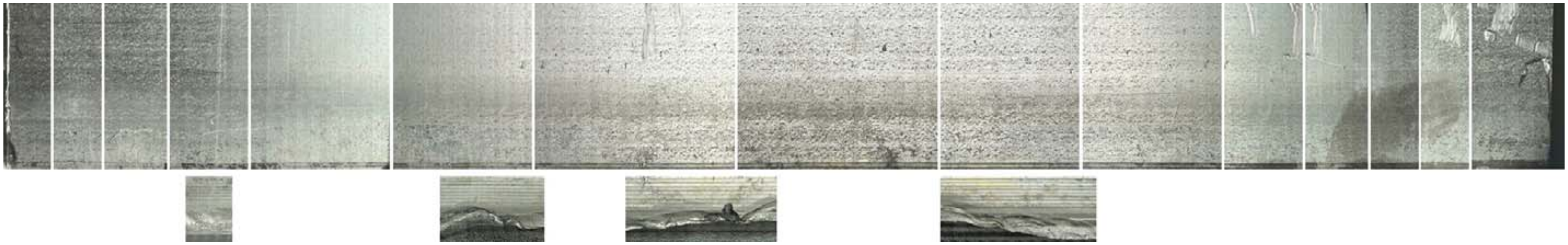

Figure B.3 Side by side LCM assemblies of Zone 3 (top) and Zones 1 and 2 (bottom) of ICCWR for FY15 DE07 Section B1. Zone 1 corresponds to the weld beads, Zone 2 corresponds to the machining marks region (above weld beads), and Zone 3 is the region above the machining marks. Each image represents an assembly of 45 to 135 individual images. Some overlap exits between assemblies to ensure data collection of 100% of full circumference.

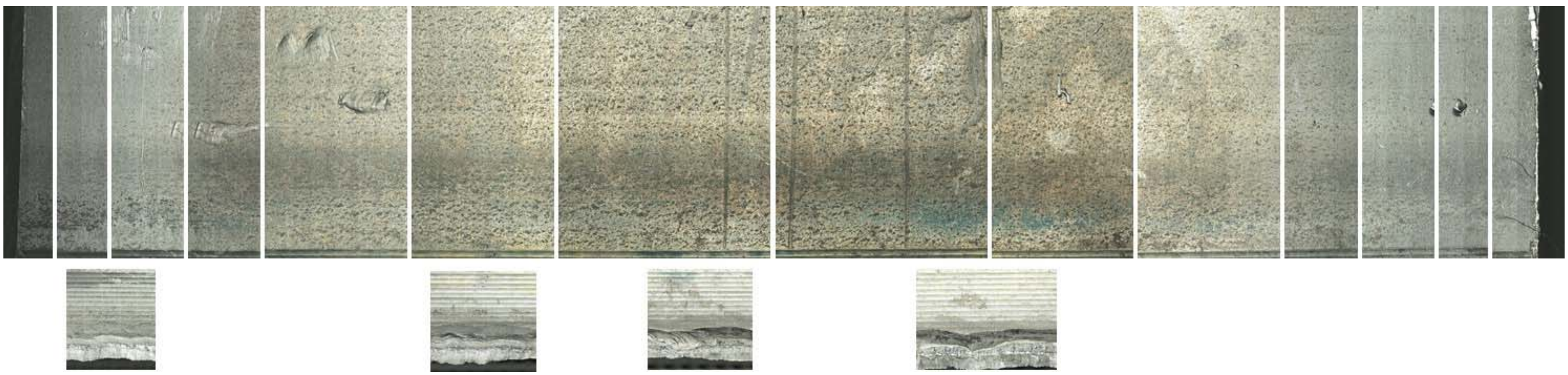

Figure B.4 Side by side LCM assemblies of Zone 3 (top) and Zones 1 and 2 (bottom) of ICCWR for FY15 DE07 Section B2. Zone 1 corresponds to the weld beads, Zone 2 corresponds to the machining marks region (above weld beads), and Zone 3 is the region above the machining marks. Each image represents an assembly of 30 to 135 individual images. Some overlap exits between assemblies to ensure data collection of 100% of full circumference.

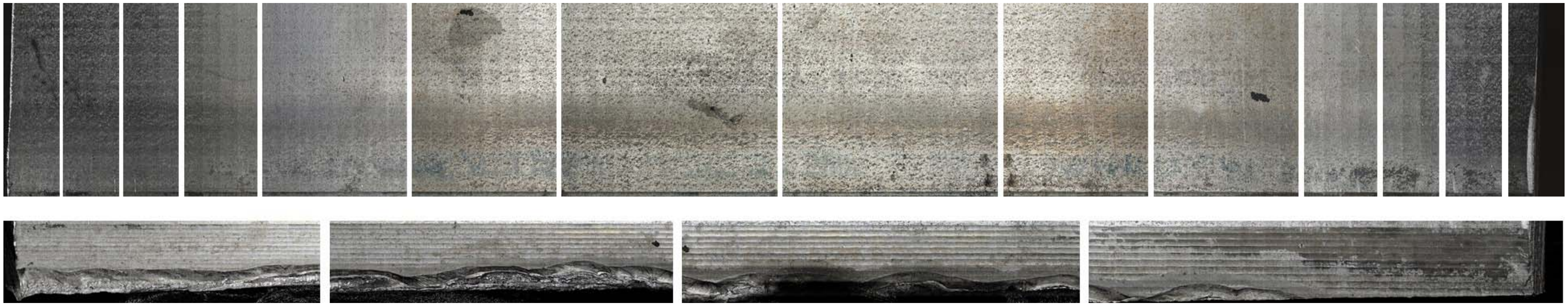

Figure B.5 Side by side LCM assemblies of Zone 3 (top) and Zones 1 and 2 (bottom) of ICCWR for FY15 DE07 Section C1. Zone 1 corresponds to the weld beads, Zone 2 corresponds to the machining marks region (above weld beads), and Zone 3 is the region above the machining marks. Each image represents an assembly of 45 to 180 individual images. Some overlap exits between assemblies to ensure data collection of 100% of full circumference.

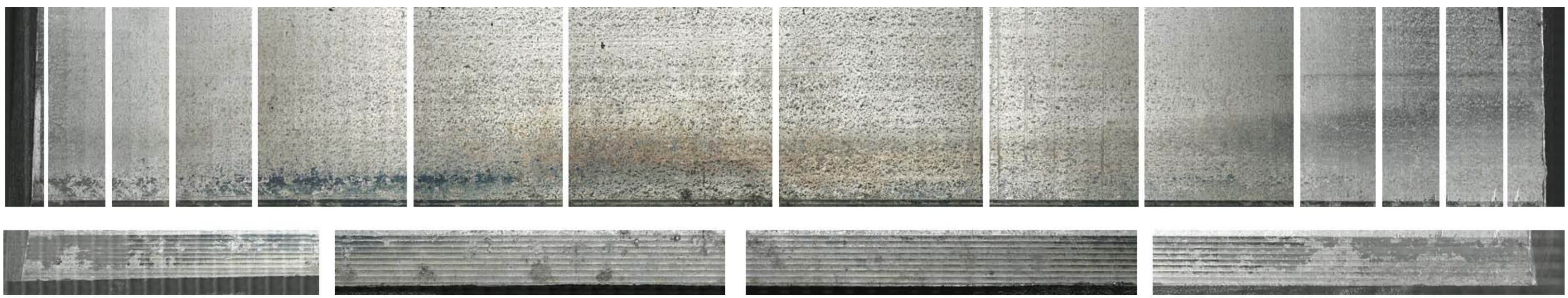

Figure B.6 Side by side LCM assemblies of Zone 3 (top) and Zones 1 and 2 (bottom) of ICCWR for FY15 DE07 Section C2. Zone 1 corresponds to the weld beads, Zone 2 corresponds to the machining marks region (above weld beads), and Zone 3 is the region above the machining marks. Each image represents an assembly of 30 to 165 individual images. Some overlap exits between assemblies to ensure data collection of 100% of full circumference.

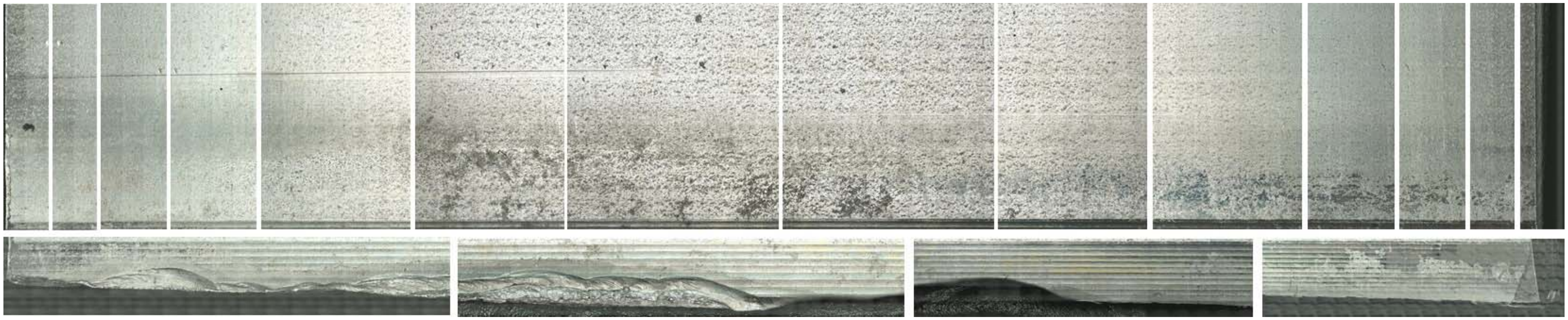

Figure B.7 Side by side LCM assemblies of Zone 3 (top) and Zones 1 and 2 (bottom) of ICCWR for FY15 DE07 Section D1. Zone 1 corresponds to the weld beads, Zone 2 corresponds to the machining marks region (above weld beads), and Zone 3 is the region above the machining marks. Each image represents an assembly of 30 to 150 individual images. Some overlap exits between assemblies to ensure data collection of 100% of full circumference.

Figure B.8 Side by side LCM assemblies of Zone 3 (top) and Zones 1 and 2 (bottom) of ICCWR for FY15 DE07 Section D2. Zone 1 corresponds to the weld beads, Zone 2 corresponds to the machining marks region (above weld beads), and Zone 3 is the region above the machining marks. Each image represents an assembly of 30 to 165 individual images. Some overlap exits between assemblies to ensure data collection of 100% of full circumference.